PAPER • OPEN ACCESS

Kinetics of recrystallization and grain growth in an ultra-fine grained CoCrFeNiMn-type high-entropy alloy

Kinetics of recrystallization and grain growth in an ultra-fine grained CoCrFeNiMn-type high-entropy alloy

M V Klimova[1], D G Shaysultanov[1], R S Chernichenko[1], V N Sanin[2], S V Zherebtsov[1] and N D Stepanov[1,*]

[1] Laboratory of Bulk Nanostructured Materials, Belgorod National Research University, Belgorod 308015, Russia
[2] Merzhanov Institute of Structural Macrokinetics and Materials Science, Russian Academy of Sciences, Chernogolovka, Moscow, 142432 Russia

Corresponding author: stepanov@bsu.edu.ru

Abstract. A novel high entropy alloy based on the CoCrFeMnNi system with substantial amounts of Al and C was studied. After cold rolling and annealing at 973-1273 K a duplex ultra-fine grained structure composed of the recrystallized fcc grains and $M_{23}C6$ and B2 particles was produced. Analysis of the coarsening behavior of grains and particles growth suggested that kinetics of both was controlled by volume diffusion. The apparent activation energy of structure coarsening during recrystallization was evaluated.

1. Introduction

The so-called high entropy alloys (HEAs), multicomponent alloys of 5 or more principal elements taken in nearly equiatomic concentration (5-35 at.%), have become a very attractive research field in materials science [1,2]. The well-known HEAs family is based on 3d transition metals like Cr, Mn, Fe, Co and Ni [3]. A typical and well-investigated representative of this family is the equiatomic CoCrFeMnNi alloy, also known as the Cantor alloy [4–7]. This alloy has a single disordered face-centered cubic (fcc) structure at temperatures >900°C [6,8–13] and is widely considered as a "model" single phase HEA. In addition, the alloy has attractive mechanical properties; namely very high ductility and fracture toughness at room temperature [5,7], which yet increases even more under cryogenic condition. Nevertheless, the strength of the alloy is quite low [5,11].

Numerous efforts have been undertaken to increase the strength of the CoCrFeMnNi and similar alloys. Precipitation hardening was found to be a particularly effective [14–16]. Compound-forming elements like Al and Ti are often used to produce strengthening precipitates. For example, after proper heat treatment, a CoCrFeNi alloy, containing 4 at.% of Al and 2 at.% of Ti, demonstrates the ultimate tensile strength of ~1100 MPa with elongation of ~40% due to strong precipitation strengthening by $L1_2$ phase particles [14]. Similarly, strong precipitation strengthening can be achieved in the alloys which are doped with carbon thanks to precipitation of fine carbide particles [16,17].

Another approach to increase the strength of the CoCrFeNiMn alloys is to refine the fcc grain size. It is well established that the CoCrFeMnNi alloy can have very high Hall-Petch coefficient, about ~0.5 $GPa \times \mu m^{-0.5}$ [5]. Indeed, some earlier reports demonstrated promising mechanical properties of the equiatomic CoCrFeMnNi alloy with the grain size of d≈0.5 μm [18,19]. In these works, cold working followed by annealing at temperatures ≥650°C was used to produce the ultra-fine grained (UFG)

structure. Because of relatively fast kinetics of recrystallization and grain growth in the single-phase CoCrFeNiMn alloy [20,21], very precise control over the annealing condition is needed for preserving the fine grain size.

A different approach to produce UFG structure was used in [22,23]. Here, the studied alloys contained substantial amounts of Al or Al and C. Presence of additional elements resulted in the precipitation of second phase particles during post-rolling annealing, that impeded the growth of the recrystallized fcc grains. As a result, duplex UFG structure providing a good balance between strength and ductility was formed. However, the stability of such a structure requires additional studies. In present work, the type and the kinetics of coarsening of second-phase precipitates and grain growth during annealing at 973-1273 K for up to 10 hours in the previously reported Al, C containing CoCrFeMnNi-type alloy [22] were determined.

2. Materials and methods

In this work, the studied alloy was fabricated via the self-propagating high-temperature synthesis (SHS)-casting technique. The initial products were taken in the form of a mixture of powders including oxides of the target elements (Co, Cr, Fe, Mn, Ni), Al (both as the metal reducer and alloying element), and pure C (graphite powder). Prior to the synthesis, the powders were mechanically mixed for 20 min. The mixture was placed in centrifuge with a graphite mold of 80 mm diameter under artificial gravity of 50-60 G.

The obtained ingot had the diameter of 40 mm and the length of 70 mm. The chemical composition of the obtained ingot is given in Table 1. Samples for the thermomechanical processing having the dimensions of $4 \times 5 \times 22$ mm^3 were cut from the as-cast ingot by an electric discharge machine were. These samples were cold rolled to the final thickness of ≈ 0.32 mm corresponding to a thickness reduction of 92% with reduction per pass of 5-10%. Cold-rolled samples were annealed at 973-1273 K for 0.5, 1, 5, and 10 hours. For the annealing, the samples were placed in a preheated oven and held for the desired durations of time; cooling was carried by air.

Table 1. Chemical composition of the studied alloy (in at.%).

Co	Cr	Fe	Mn	Ni	Al	C
21.55	18.73	21.44	10.01	21.44	5.31	1.52

Microstructures of the annealed alloy were studied by scanning (SEM) electron microscopy mainly. The samples for scanning electron microscopy were prepared by careful mechanical polishing. The SEM studies were performed using a FEI Quanta 600 FEG microscope equipped with backscattered electron (BSE) and energy dispersive spectrometry (EDS) detectors. The grain/particle size was measured using SEM-BSE images per standard linear interception method. At least 300 grains/particles per each condition were analyzed. The fraction of the second phase(s) was measured from SEM-BSE images using a commercial Digimizer Image Analysis software and a binarization procedure. To identify the crystallographic structure of different phases, transmission electron microscopy (TEM) was employed. Details on TEM procedures can be found elsewhere [22].

3. Results

Cold rolling and annealing in the interval of 973-1273 K resulted in the formation of a duplex ultrafine-grained structure composed of the recrystallized fcc grains and $M_{23}C_6$ type carbides and B2 particles (see more details in [22]). The measured chemical composition of the fcc phase has retained rather close to the nominal one (Table 1), however it was depleted of Al and enriched in Co and Fe (~24-26 at.% each). The carbides were primarily composed of Cr (≈ 63 at.%), and depleted of other metallic elements. The B2 phase, in turn, was enriched with Ni (~35-37 at.%), Mn (~14-17 at.%), and Al (~14-21 at.%), and depleted of the rest of the elements. Since the clear distinction between the morphology of the particles was not possible, the size and the fraction of the $M_{23}C_6$ and B2 second phase's particles were measured jointly.

The effect of annealing temperature or time on the hardness of cold rolled samples is shown in Figure 1. Annealing at 973 K for 0.5 or 1 hour leads to a slight increase in hardness from 478 HV (in the cold-rolled state) to 513 or 495 HV. Such hardening may be due to the formation of second phase particles in a non-recrystallized or partially recrystallized state [13]. However, a further increase in the annealing temperature or time resulted in a remarkable decrease in the hardness in all interval of annealing times which associated with primary static recrystallization.
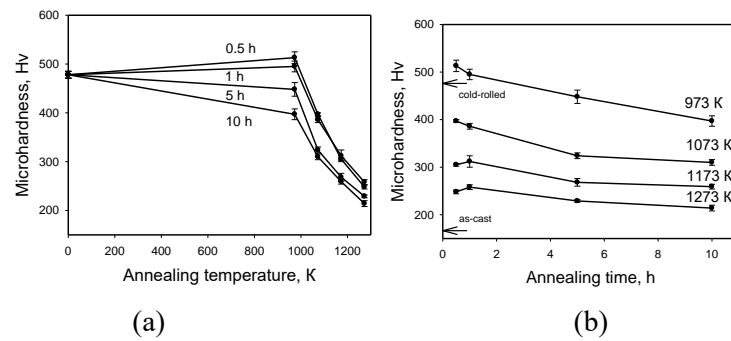

Figure 1. Effect of annealing temperature (a) and time (b) on the microhardness of the Al, C-containing CoCrFeMnNi-type alloy.

Typical microstructures, which formed in the cold rolled samples after annealing for 0.5 or 10 hours at temperatures of 973-1273 K, are shown in Figure 2. Annealing of the rolled alloy during 0.5 h at temperatures 973 - 1073 K resulted in partial recrystallization of the fcc matrix phase (Figure 2 a, b). The corresponding microstructures consisted of deformed areas and equiaxed recrystallized grains. An increase in the annealing temperature to 1173-1273 K gave rise to complete recrystallization (Figure 2 c, d). After annealing at 973 K the recrystallized fraction and the size of the recrystallized grains were 0.52 and 0.57±0.23 μm, respectively (Table 2). An increase in the annealing temperature to 1273 K resulted in an increase in grain size to 1.75±0.85 μm.
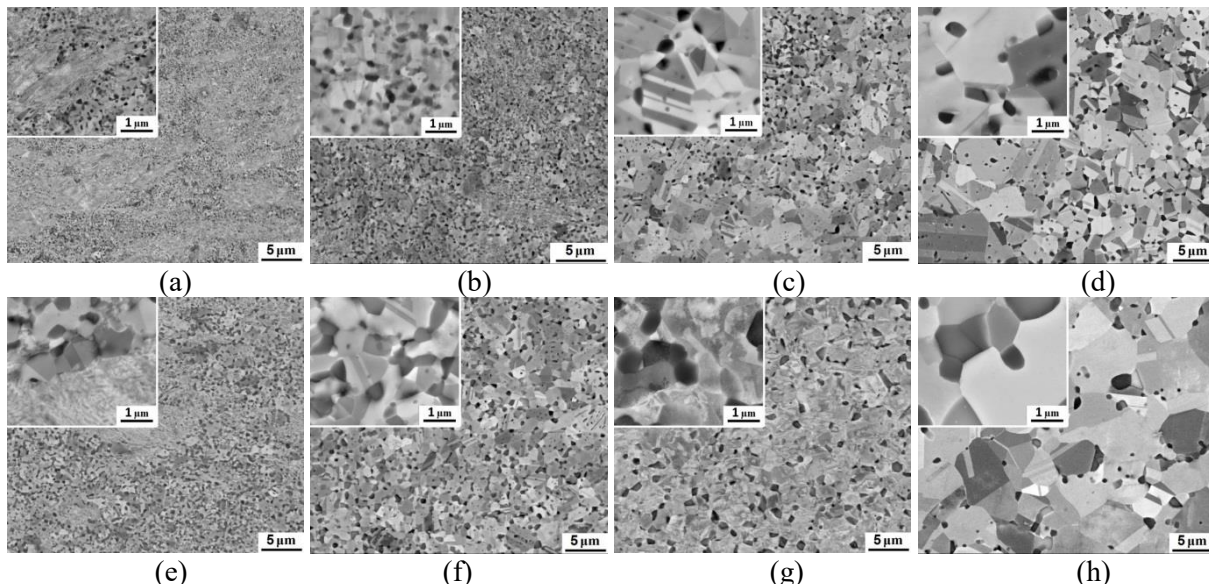

Figure 2. SEM-BSE images of the alloy after cold rolling to 92% thickness reduction and subsequent annealing for 0.5 h (a-d) and 10 h (e-h) at (a, e) – 973 K, (b, f) – 1073 K, (c, g) – 1173 K, (d, h) – 1273 K.

It is worth noting that an increase in the annealing time to 10 hours at the temperature of 973 K does not lead to the formation of a fully recrystallized structure (Figure 2e). The average grain size in the

recrystallized microstructures increased with an increase in the annealing time (Table 2). A number of equilibrium triple junctions of grain boundaries (120° between boundaries in triple junctions) indicates normal grain growth as the main mechanism of microstructure evolution. The growing grains are characterized by numerous annealing twins, which are typical of low SFE metals and alloys during recrystallization followed by normal grain growth.

The grain growth takes place concurrently with the carbide and B2 particles coarsening. In the partially recrystallized condition the second phases were predominantly found in the recrystallized regions. The particles located at the grain boundaries were generally coarser than the particles inside recrystallized grains. The estimated fraction of the second phases decreased with increasing of annealing time and temperature at 1073-1273 K. A nonlinear dependence of the fraction of the particles at low annealing temperature can be associated with the development of primary recrystallization, when particle formation occurs in recrystallized regions. On the other hand, the average size of the second phase's particles increased from 0.14±0.05 μm to 0.53±0.27 μm when temperature increased from 973 K to 1273 K.

Table 2. Microstructure parameters of the studied alloy after cold rolling to 92% thickness reduction and subsequent annealing at 973 K, 1073 K, 1173 K, and 1273 K for 0.5-10 hours.

Temperature	973 K				1073 K				1173 K				1273 K			
Time, h	0.5	1	5	10	0.5	1	5	10	0.5	1	5	10	0.5	1	5	10
Grain size, μm	0.57 ± 0.23	0.42 ± 0.16	0.84 ± 0.31	1.10 ± 0.52	0.55 ± 0.22	0.88 ± 0.42	1.00 ± 0.36	1.41 ± 0.65	1.03 ± 0.35	0.90 ± 0.31	1.81 ± 0.65	1.85 ± 0.44	1.75 ± 1.15	2.28 ± 1.05	3.10 ± 1.36	4.69 ± 2.40
Particle size, nm	136 ± 52	165 ± 66	246 ± 122	294 ± 114	240 ± 100	258 ± 117	314 ± 183	416 ± 212	299 ± 160	356 ± 156	459 ± 268	542 ± 231	530 ± 270	465 ± 217	967 ± 435	935 ± 459
Particles fraction, %	5.9	9.6	20.2	10.6	19.9	15.2	13.7	9.4	17.3	12.9	7.85	6.5	14.1	8.16	6.0	3.5

The kinetics of the grain/precipitate coarsening was well described by the power-law dependence:

$$d^n - d_0^n = Kt \qquad (1)$$

where n is the grain/particle growth exponents, d_o is grain/particle size, and K is the rate constant at a given temperature. The exponent n =3 suggests that coarsening was controlled by volume diffusion (Figure 3 a, b).

The temperature dependence of the grain size is given by the dependence of rate constant K on temperature, Eq. (1), which has an Arrhenius form:

$$K = K_0 \exp(-Q/RT) \qquad (2)$$

Here, T is the absolute temperature, Q is the apparent activation energy for grain/particle growth, R is the gas constant, and K_o is a material constant. The apparent activation energy was calculated from the linear dependence of ln(K) on 1/T (Figure 3c). In particular, the present analysis showed that Q = 137 kJ/mol for grain growth and Q = 125 kJ/mol for particles coarsening. The obtained values are considerably lower than that were reported for bulk self-diffusion of constitutive elements of the CoCrFeMn$_{0.5}$Ni alloy (288.4-317.5 kJ/mol) [24]. Note that the information on diffusion behavior of Al and C in the fcc HEAs are currently lacking, yet the self-diffusion energies of these species in γ (fcc) Fe are ~300 kJ/mol [25,26]. Therefore, additional work is required to correlate the obtained values of activation energies of grain growth/particles coarsening with the responsible mechanisms. This work will be performed in future studies.
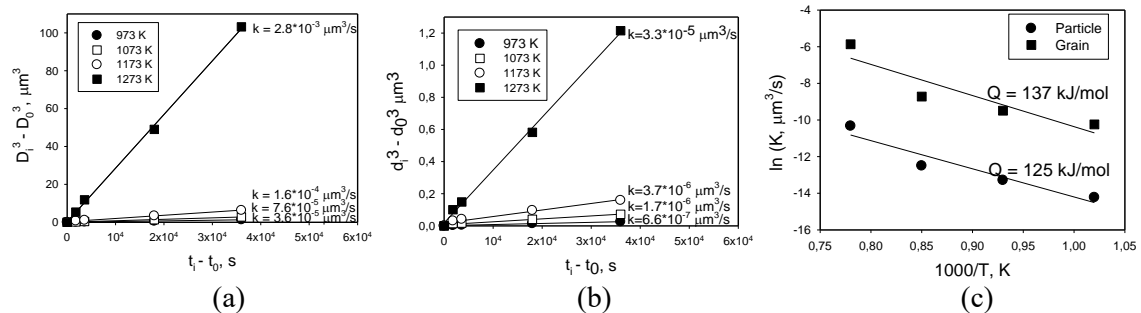
Figure 3. Dependence of (a) the fcc grain and (b) particles size on annealing time during annealing at 973-1273 K and (c) Arrhenius plots describing the apparent activation energy for grain or particle growth.

4. Conclusions

In the present work, recrystallization and grain growth of the CoCrFeMnNi-type high entropy alloy with subsequent annealing at 973-1273 K were studied. Following conclusions were drawn:

1) The annealed alloy is composed of the fcc matrix phase with the presence of B2 and M23C6 particles. Fraction and size of recrystallized fcc grains and size of the second phase particles increased with the increase of the annealing temperature, while the fraction of second phase particles exhibited complex dependence on annealing conditions.

2) Power law-type dependence between the grain/particle size and annealing time was observed. The exponent value of n=3 suggested that coarsening was controlled by volume diffusion. The activation energy was Q = 137 kJ/mol for grain growth and Q = 125 kJ/mol for particles coarsening.

References

[1]   Yeh J W, Chen S K, Lin S J, Gan J Y, Chin T S, Shun T T, Tsau C H and Chang S Y 2004 Nanostructured high-entropy alloys with multiple principal elements: Novel alloy design concepts and outcomes *Adv. Eng. Mater.* **6** 299–303+274

[2]   Senkov O N, Scott J M, Senkova S V., Miracle D B and Woodward C F 2011 Microstructure and room temperature properties of a high-entropy TaNbHfZrTi alloy *J. Alloys Compd.* **509** 6043–8

[3]   Miracle D B and Senkov O N 2017 A critical review of high entropy alloys and related concepts *Acta Mater.* **122** 448–511

[4]   Cantor B, Chang I T H, Knight P and Vincent A J B 2004 Microstructural development in equiatomic multicomponent alloys *Mater. Sci. Eng. A* **375** 213–8

[5]   Otto F, Dlouhý A, Somsen C, Bei H, Eggeler G and George E P 2013 The influences of temperature and microstructure on the tensile properties of a CoCrFeMnNi high-entropy alloy *Acta Mater.* **61** 5743–55

[6]   Otto F, Yang Y, Bei H and George E P P 2013 Relative effects of enthalpy and entropy on the phase stability of equiatomic high-entropy alloys *Acta Mater.* **61** 2628–38

[7]   Gludovatz B, Hohenwarter A, Catoor D, Chang E H, George E P and Ritchie R O 2014 A fracture-resistant high-entropy alloy for cryogenic applications *Science (80-.).* **345** 1153–8

[8]   Schuh B, Mendez-Martin F, Völker B, George E P, Clemens H, Pippan R and Hohenwarter A 2015 Mechanical properties, microstructure and thermal stability of a nanocrystalline CoCrFeMnNi high-entropy alloy after severe plastic deformation *Acta Mater.* **96** 258–68

[9]   Otto F, Dlouhý A, Pradeep K G, Kuběnová M, Raabe D, Eggeler G and George E P 2016 Decomposition of the single-phase high-entropy alloy CrMnFeCoNi after prolonged anneals at intermediate temperatures *Acta Mater.* **112**

[10]   Stepanov N D, Shaysultanov D G, Ozerov M S, Zherebtsov S V. and Salishchev G A 2016

Second phase formation in the CoCrFeNiMn high entropy alloy after recrystallization annealing *Mater. Lett.* **185** 1–4

[11]   Salishchev G A, Tikhonovsky M A, Shaysultanov D G, Stepanov N D, Kuznetsov A V, Kolodiy I V, Tortika A S and Senkov O N 2014 Effect of Mn and v on structure and mechanical properties of high-entropy alloys based on CoCrFeNi system *J. Alloys Compd.* **591** 11–21

[12]   Laurent-Brocq M, Akhatova A, Perrière L, Chebini S, Sauvage X, Leroy E and Champion Y 2015 Insights into the phase diagram of the CrMnFeCoNi high entropy alloy *Acta Mater.* **88**

[13]   Klimova M V, Shaysultanov D G, Zherebtsov S V and Stepanov N D 2019 Effect of second phase particles on mechanical properties and grain growth in a CoCrFeMnNi high entropy alloy *Mater. Sci. Eng. A* **748** 228–35

[14]   He J Y, Wang H, Huang H L, Xu X D, Chen M W, Wu Y, Liu X J, Nieh T G, An K and Lu Z P 2016 A precipitation-hardened high-entropy alloy with outstanding tensile properties *Acta Mater.* **102** 187–96

[15]   Gwalani B, Soni V, Lee M, Mantri S, Ren Y and Banerjee R 2017 Optimizing the coupled effects of Hall-Petch and precipitation strengthening in a Al0.3CoCrFeNi high entropy alloy *Mater. Des.* **121** 254–60

[16]   Klimova M V., Shaysultanov D G, Chernichenko R S, Sanin V N, Stepanov N D, Zherebtsov S V. and Belyakov A N 2019 Recrystallized microstructures and mechanical properties of a C-containing CoCrFeNiMn-type high-entropy alloy *Mater. Sci. Eng. A* **740–741** 201–10

[17]   Stepanov N D, Yurchenko N Y, Tikhonovsky M A and Salishchev G A 2016 Effect of carbon content and annealing on structure and hardness of the CoCrFeNiMn-based high entropy alloys *J. Alloys Compd.* **687** 59–71

[18]   Sun S J, Tian Y Z, Lin H R, Dong X G, Wang Y H, Zhang Z J and Zhang Z F 2017 Enhanced strength and ductility of bulk CoCrFeMnNi high entropy alloy having fully recrystallized ultrafine-grained structure *Mater. Des.* **133** 122–7

[19]   Wang Y H, Zhang Z F, Sun S J, Yang H J, Tian Y Z, Lin H R and Dong X G 2017 Transition of twinning behavior in CoCrFeMnNi high entropy alloy with grain refinement *Mater. Sci. Eng. A* **712** 603–7

[20]   Otto F, Hanold N L and George E P 2014 Microstructural evolution after thermomechanical processing in an equiatomic, single-phase CoCrFeMnNi high-entropy alloy with special focus on twin boundaries *Intermetallics* **54** 39–48

[21]   Liu W H, Wu Y, He J Y, Nieh T G and Lu Z P 2013 Grain growth and the Hall-Petch relationship in a high-entropy FeCrNiCoMn alloy *Scr. Mater.* **68** 526–9

[22]   Stepanov N D, Shaysultanov D G, Chernichenko R S, Ikornikov D M, Sanin V N and Zherebtsov S V. 2018 Mechanical properties of a new high entropy alloy with a duplex ultra-fine grained structure *Mater. Sci. Eng. A* **728** 54–62

[23]   Yasuda H Y, Miyamoto H, Cho K and Nagase T 2017 Formation of ultrafine-grained microstructure in Al0.3CoCrFeNi high entropy alloys with grain boundary precipitates *Mater. Lett.* **199** 120–3

[24]   Tsai K-Y, Tsai M-H and Yeh J-W 2013 Sluggish diffusion in Co–Cr–Fe–Mn–Ni high-entropy alloys *Acta Mater.* **61** 4887–97

[25]   Vasilyev A A, Sokolov S F, Kolbasnikov N G and Sokolov D F 2011 Effect of alloying on the self-diffusion activation energy in γ-iron *Phys. Solid State* **53** 2194–200

[26]   Zhang B 2014 Calculation of self-diffusion coefficients in iron *AIP Adv.* **4** 017128

Acknowledgments